Manuscript prepared for Atmos. Chem. Phys.
with version 4.2 of the LaTeX class copernicus.cls.
Date: 22 October 2013

Analysis of the Effect of Water Activity on Ice Formation using a New Theory of Nucleation

D. Barahona

Global Modeling and Assimilation Office, NASA Goddard Space Flight Center, Greenbelt, Maryland, USA

Correspondence to: D. Barahona (donifan.o.barahona@nasa.gov)

Abstract. In this work a new theory of nucleation is developed and used to investigate the effect of water activity on the formation of ice within supercooled droplets. The new theory is based on a novel concept where the interface is assumed to be made of liquid molecules "trapped" by the solid matrix. Using this concept new expressions are developed for the critical ice germ size and the nucleation work, with explicit dependencies on temperature and water activity. However unlike previous approaches, the new theory does not depend on the interfacial tension between liquid and ice. Comparison against experimental results shows that the new theory is able to reproduce the observed effect of water activity on nucleation rate and freezing temperature. It allows for the first time a theoretical derivation of the constant shift in water activity between melting and nucleation. The new theory offers a consistent thermodynamic view of ice nucleation, simple enough to be applied in atmospheric models of cloud formation.

1 Introduction

Ice formation by freezing of supercoooled droplets is an important natural and technological process. In the atmosphere it leads to the formation of cirrus and determines the freezing level of convective clouds (Pruppacher and Klett, 1997). At temperatures below 238 K and in the absence of ice forming nuclei, freezing proceeds by homogeneous nucleation. A significant fraction of cirrus in the upper troposphere forms by this mechanism (Gettelman et al., 2012; Barahona et al., 2013). Cirrus clouds impact the radiative balance of the upper troposphere (Fu, 1996) and play a role in the transport of water vapor to the lower stratosphere (e.g., Barahona and Nenes, 2011; Jensen and Pfister, 2004; Hartmann et al., 2001). Correct parameterization of ice formation is therefore crucial for reliable climate and weather prediction (Lohmann and Feichter, 2005). Many experimental and theoretical studies have been devoted to the study of homogeneous nucleation (e.g., Kashchiev, 2000; Murray

et al., 2010b; Wu et al., 2004, and references therein), yet there are still significant gaps in the understanding of ice formation within supercooled droplets.

The theoretical study of homogeneous ice nucleation is commonly approached by using the Classical Nucleation Theory (CNT) (e.g., Khvorostyanov and Curry, 2004) or by molecular dynamics (MD) simulations (e.g., Matsumoto et al., 2002). Density functional theory and direct kinetic models have also been employed (Laaksonen et al., 1995). MD and other detailed approaches offer a unique look to the microscopic mechanism of ice nucleation. However, for climate simulations simplified and efficient descriptions of ice nucleation are required. Thus CNT is typically used to generate ice formation parameterizations in atmospheric models (Liu and Penner, 2005; Khvorostyanov and Curry, 2004).

CNT is often criticized due to the usage of the so-called capillary approximation, i.e., the assumption that the properties of ice clusters at nucleation are the same as those of the bulk (Kashchiev, 2000). Among the parameters used by CNT, the ice-liquid interfacial tension (also called specific surface energy), σ_{iw}, is generally the most uncertain. CNT predictions are highly sensitive to σ_{iw}, however direct measurements of σ_{iw} are typically difficult and are only available at low supercooling (Pruppacher and Klett, 1997). Furthermore, other factors not considered by CNT like crystal shape, type and size, and the lack of a well-defined ice liquid interface may also play a role in determining σ_{iw} (Wu et al., 2004; MacKenzie, 1997; Kashchiev, 2000; Murray et al., 2010a). Thus σ_{iw} is often found by fitting to CNT predictions to experimental measurements of the nucleation rate (Murray et al., 2010a; Khvorostyanov and Curry, 2004). The caveat is that σ_{iw} obtained by this method often differs significantly from theoretical estimates (MacKenzie, 1997), casting doubt into the validity of CNT.

Due to the shortcomings of CNT, experimental data are most often used to describe homogeneous freezing in atmospheric models (e.g., Barahona and Nenes, 2008; Kärcher and Lohmann, 2002). Experimental studies generally agree on the freezing temperature of pure water with typical variation below one degree (Murray et al., 2010a; Pruppacher and Klett, 1997). For liquid solutions this picture is somewhat complicated by the chemical heterogeneity of liquid droplets in the atmosphere. Empirical correlations were often developed based on $(NH_4)_2SO_4$ and H_2SO_4 model solutions (e.g., Tabazadeh et al., 1997; Jensen et al., 1991). This issue was resolved by Koop et al. (2000) who demonstrated that when parameterized in terms of the water activity, a_w, freezing temperatures are independent of the nature of the solute. Furthermore, the authors showed that when plotted in a $T - a_w$ diagram, the melting and nucleation curves can be translated by a constant shift in water activity. This finding has been confirmed by several independent studies (Marcolli et al., 2007; Wang and Knopf, 2011) and has been be referred to as the "water activity criteria". The Koop et al. (2000) (hereafter K00) parameterization has been incorporated in several global atmospheric models (e.g., Barahona et al., 2010; Liu et al., 2007).

The study of Koop et al. (2000) suggested that a general thermodynamic formulation of ice nucle-

ation could be achieved, however such theory has been so far elusive. Current formulations of CNT carry a dependency on a_w and it has been suggested that CNT can explain the water activity criteria (e.g., Khvorostyanov and Curry, 2004). However in these studies σ_{iw} is typically modified to adjust CNT to K00, therefore the results obtained in this way are not independent of Koop et al. (2000) data. In fact, Koop et al. (2000) suggested that CNT and K00 can be reconciled if σ_{iw} is allowed to vary with a_w, although no theoretical support was provided for it. Baker and Baker (2004) took an alternative approach and showed that the freezing temperatures measured by K00 were consistent with the point of maximum compressibility of water. The authors derived an empirical relation between a_w and the osmotic pressure which was then to used to determine freezing temperatures. The work of Baker and Baker (2004) demonstrated that the water activity criteria can be understood in terms of water compressibility as long as certain empirical criteria are met. However a theoretical basis for this behavior was not provided. Furthermore, the liquid-only approach used by the authors is in contrast with MD simulations showing that ice nucleation originates in differentiated, ice-like regions within the liquid phase (Matsumoto et al., 2002).

In this work a new approach is proposed to describe ice formation by homogeneous nucleation. The new model relies on a novel picture of the solid-liquid transition placing emphasis on the entropy changes across the interface. The new model is used to analyze the effect of water activity on ice formation and ice nucleation rates.

2 Theory

Consider the system of Fig. 1. The liquid droplet is assumed to be large enough so that nucleation is more likely to occur within the bulk of the liquid than at the droplet surface. The liquid is assumed to be homogeneously mixed and its cluster distribution in steady state. For simplicity it is assumed that only two components are present in solution, water (subscript, "w") and a solute (subscript, "y"), although this assumption can be easily relaxed if more than one solute is present. The Gibbs free energy of the system in stage 1 (before germ formation) is given by

$$G_1 = N_w \mu_{w,1} + N_y \mu_{y,1} \tag{1}$$

where N_w and N_y are the total number of water and solute molecules present in the liquid phase, respectively, and $\mu_{w,1}$ and $\mu_{y,1}$ their respective chemical potentials.

After the formation of the germ (stage 2, Fig. 1) it is advantageous to consider the solid-liquid interface as a phase distinct from the bulk (Gibbs et al., 1928). It is assumed that no atoms of y are present in the bulk of the solid phase although they may be present at the interface. However the dividing surface is selected so that the molecular excess of solute at the interface is zero (this is further analyzed in Section 2.1). The assumption of a solute-free solid is justified on molecular dynamics simulations showing a rejection of ions into a unfrozen layer of brine away from the germ

(Bauerecker et al., 2008). With this, the Gibbs free energy of the system in stage 2 is given by

$$G_2 = (N_w - n_s - n_{ls})\mu_{w,2} + N_y\mu_{y,2} + n_s\mu_{w,s} + n_{ls}\mu_{w,ls} \tag{2}$$

where n_s and n_{ls} are the number of atoms in the bulk of the germ and in the interface, respectively, and $\mu_{w,s}$ and $\mu_{w,ls}$, their chemical potentials. Equation (2) can be reorganized as,

$$G_2 = N_w\mu_{w,2} + N_y\mu_{y,2} + n_s(\mu_{w,s} - \mu_{w,2}) + n_{ls}(\mu_{w,ls} - \mu_{w,2}) \tag{3}$$

Using Eqs. (1) and (3) the work of germ formation, $\Delta G = G_2 - G_1$, can be written as

$$\Delta G = \Delta G_{\rm sln} + n_s(\mu_{w,s} - \mu_{w,2}) + n_{ls}(\mu_{w,ls} - \mu_{w,2}) \tag{4}$$

where $\Delta G_{\rm sln}$ is the change in the Gibbs free energy of the bulk solution caused by the appearance of the germ, i.e.,

$$\Delta G_{\rm sln} = N_w(\mu_{w,2} - \mu_{w,1}) + N_y(\mu_{y,2} - \mu_{y,1}) \tag{5}$$

Eq. (4) indicates that the work of germ formation originates from (i) changes in the composition of the liquid phase, (ii) the formation of the interface and (iii) the formation of the bulk of the solid. Using the equilibrium between ice and the liquid solution as reference state, the latter can be written in the form (Kashchiev, 2000),

$$\mu_{w,s} - \mu_{w,2} = -k_{\rm B}T\ln\left(\frac{a_w}{a_{w,eq}}\right) \tag{6}$$

where $k_{\rm B}$ is the Boltzmann constant and $a_{w,eq}$ is the equilibrium water activity between bulk liquid and ice.

$\Delta G_{\rm sln}$ in Eq. (5) arises because the solute must be "unmixed" (Black, 2007) from the liquid to form a solute-free germ, causing a change in the molar composition of the liquid phase. Such unmixing carries an entropic cost to the system (Bourne and Davey, 1976). Thus, $\Delta G_{\rm sln}$ is proportional to the mixing entropy of the atoms in the germ,

$$\Delta G_{\rm sln} = -nk_{\rm B}T(X_w\ln a_w - X_y\ln a_y) \tag{7}$$

Where X_w and X_y are the molar fractions of water and solute in the bulk liquid, respectively. For dilute solutions, which is almost always the case for ice nucleation, $X_w >> X_y$ and,

$$\Delta G_{\rm sln} \approx -nk_{\rm B}T\ln a_w \tag{8}$$

Where $n = n_s + n_{ls}$ is the total number of molecules in the germ.

2.1 Energy of formation of the interface

To further develop Eq. (4) it is necessary to introduce a model of the solid-liquid interface. Theoretical models show that the solid-liquid interface is characterized by the organization of randomly moving liquid molecules into positions determined by the solid matrix (Spaepen, 1975; Karim and Haymet, 1988; Haymet and Oxtoby, 1981). Associated with this increased order is a decrease in the partial molar entropy of the liquid molecules. Since the solid determines the positions of the molecules at the interface, the partial molar entropy at the interface must approximate the bulk entropy of the solid. However the interface molecules are liquid-like, and their enthalpy remains that of the bulk liquid (Black, 2007). This implies that the system must pay the maximum entropic cost during the formation of the germ (Spaepen, 1975; Black, 2007). The entropic nature of the thermodynamic barrier for nucleation has been confirmed by molecular dynamics simulations (Reinhardt and Doye, 2013). This conceptual model is used below to develop an expression for the energy of formation of the interface.

The change in the partial molar free energy of water associated with the formation of the interface is given by

$$\mu_{w,ls} - \mu_{w,2} = h_{w,ls} - Ts_{w,ls} - \mu_{w,2} \tag{9}$$

Where $s_{w,ls}$ is the entropy of the interface molecules. Assuming that the entropy of the molecules at the interface approximates the entropy of the bulk solid, i.e., $s_{w,ls} \approx s_{w,s}$, Eq. (9) can be written as,

$$\mu_{w,ls} - \mu_{w,2} = h_{w,ls} - Ts_{w,s} - \mu_{w,2} \tag{10}$$

Taking into account that $\mu_{w,s} = h_{w,s} - Ts_{w,s}$, and using Eq. (6) into Eq. (10) we obtain

$$\mu_{w,ls} - \mu_{w,2} = -k_{\mathrm{B}}T\ln\left(\frac{a_w}{a_{w,eq}}\right) + \Delta h_{w,ls} \tag{11}$$

where $\Delta h_{w,ls} = h_{w,ls} - h_{w,s}$ is the excess enthalpy of the molecules at the interface.

If no solute is present the enthalpy of the molecules at the interface approximates the enthalpy of water in the bulk, i.e, $\Delta h_{w,ls} \approx \Delta h_f$ where Δh_f is the latent heat of fusion of water. However the adsorption of solute at the interface affects $\Delta h_{w,ls}$. Using the Gibbs model of adsorption the effect of the solute on $\Delta h_{w,ls}$ can be accounted for in the form (Hiemenz and Rajagopalan, 1997; Gibbs et al., 1928),

$$\Delta h_{w,ls} = \Delta h_f - \Gamma_w k_{\mathrm{B}}T\ln a_w - \Gamma_y k_{\mathrm{B}}T\ln a_y \tag{12}$$

where Γ_w and Γ_y are the surface excess of water and solute, respectively, and represent the ratio of the number of molecules in the interface to the number of molecules at the dividing surface. According to the Gibbs model, Γ_w and Γ_y depend on the position of the dividing surface, typically

chosen so that the surface excess of solvent is zero (Kashchiev, 2000). However by choosing the dividing surface as equimolecular with respect to the solute (Section 2) the resulting expressions become independent of the nature of the solute. Thus making $\Gamma_y = 0$, Eq. (12) becomes,

$$\Delta h_{w,ls} = \Delta h_f - \Gamma_w k_\mathrm{B} T \ln a_w \tag{13}$$

In the solid matrix the number of molecules at the surface is given by $sn^{2/3}$ where s is a geometric constant depending on the crystal lattice (1.12 for hcp crystals and 1.09 for bcc crystals (Jian et al., 2002)), and n is the total number of atoms in the germ. However the interface is generally made of several layers beyond the outer layer of the solid (Henson and Robinson, 2004; Chen and Crutzen, 1994; Spaepen, 1975). Spaepen (1975) showed that for random coverage of a solid matrix there are about 1.46 molecules at the interface for each molecule in the outer layer of the solid matrix. With this, $\Gamma_w = 1.46s$ and $n_{ls} = 1.46sn^{2/3}$. Equation (13) then becomes,

$$\Delta h_{w,ls} = \Delta h_f - 1.46 s k_\mathrm{B} T \ln a_w \tag{14}$$

Introducing Eq. (14) into Eq. (11) we obtain,

$$\mu_{w,ls} - \mu_{w,2} = -k_\mathrm{B} T \ln\left(\frac{a_w}{a_{w,eq}}\right) + \Delta h_f - 1.46 s k_\mathrm{B} T \ln a_w \tag{15}$$

Equation (15) expresses the energy cost associated with the formation of the interface accounting for solute effects. Since it results from the consideration of the maximum entropy increase across interface, this model will be referred to as the Neg-Entropic Nucleation Theory (NENT).

2.2 Nucleation work

Introducing Eqs. (6), (8) and (15) into Eq. (4), and rearranging we obtain

$$\Delta G = -n k_\mathrm{B} T \ln\left(\frac{a_w^2}{a_{w,eq}}\right) + 1.46 s n^{2/3} (\Delta h_f - 1.46 s k_\mathrm{B} T \ln a_w) \tag{16}$$

where $n = n_s + n_{ls}$ was used.

The germ size at nucleation, n^*, and the nucleation work, ΔG_nuc, are obtained by applying the condition of mechanical equilibrium to Eq. (16), i.e.,

$$\frac{\mathrm{d}\Delta G_\mathrm{nuc}}{\mathrm{d}n*} = -k_\mathrm{B} T \ln\left(\frac{a_w^2}{a_{w,eq}}\right) + \frac{2}{3} 1.46 s (n^*)^{-1/3} (\Delta h_f - 1.46 s k_\mathrm{B} T \ln a_w) = 0 \tag{17}$$

Solving Eq. (17) for n^* and rearranging gives,

$$n^* = \frac{8}{27}\left[\frac{1.46 s (\Delta h_f - 1.46 s k_\mathrm{B} T \ln a_w)}{k_\mathrm{B} T \ln\left(\frac{a_w^2}{a_{w,eq}}\right)}\right]^3 \tag{18}$$

The nucleation work is obtained by replacing Eq. (18) into Eq. (16). After rearranging we obtain,

$$\Delta G_{\rm nuc} = \frac{4}{27}\frac{\left[1.46s(\Delta h_f - 1.46sk_{\rm B}T\ln a_w)\right]^3}{\left[k_{\rm B}T\ln\left(\frac{a_w^2}{a_{w,eq}}\right)\right]^2} \tag{19}$$

The nucleation rate, $J_{\rm hom}$, is given by,

$$J_{\rm hom} = J_0 \exp\left(-\frac{\Delta G_{\rm nuc}}{k_{\rm B}T}\right) \tag{20}$$

where J_0 is a T-dependent preexponential factor. As in CNT, it is assumed that J_0 results from the kinetics of aggregation of single water molecules to the ice germ from an equilibrium cluster population (Kashchiev, 2000), therefore,

$$J_0 = \frac{N_c k_{\rm B}T}{h}\frac{\rho_w}{\rho_i}\frac{Z\Omega_g}{v_w}\exp\left(-\frac{\Delta G_{\rm act}}{k_{\rm B}T}\right) \tag{21}$$

where N_c is the number of atoms in contact with the ice germ, ρ_w and ρ_i are the bulk liquid water and ice density, respectively, Ω_g is the germ surface area, and $\Delta G_{\rm act}$ is the activation energy of the water molecules in the bulk of the liquid. Z is the Zeldovich factor, given by

$$Z = \left(\frac{\Delta G_{\rm nuc}}{3\pi k_{\rm B}Tn^*}\right)^{1/2} \tag{22}$$

2.3 Classical Nucleation Theory

CNT is commonly used to described homogeneous ice nucleation (Khvorostyanov and Curry, 2004) and is therefore important to compare the NENT model against CNT predictions. According to CNT, the nucleation rate is given by (Pruppacher and Klett, 1997) ,

$$J_{\rm CNT} = \frac{2N_c k_{\rm B}T}{h}\frac{\rho_w}{\rho_i}\left(\frac{\sigma_{iw}}{k_{\rm B}T}\right)^{1/2}\exp\left[-\frac{\Delta G_{\rm act}+\Delta G_{\rm CNT}}{k_{\rm B}T}\right] \tag{23}$$

The work of nucleation, $\Delta G_{\rm CNT}$, is calculated as

$$\Delta G_{\rm CNT} = \frac{16\pi\sigma_{iw}^3 v_w^2}{3(k_{\rm B}T\ln S_i)^2} \tag{24}$$

where $S_i = a_w(p_{\rm s,w}/p_{\rm s,i})$, is the saturation ratio with respect to the ice phase. The critical germ size is given by,

$$n^*_{\rm CNT} = \frac{32\pi\sigma_{\rm iw}^3 v_w^2}{3(k_{\rm B}T\ln S_i)^3} \tag{25}$$

The usage Eq. (23) requires a parameterization of $\sigma_{\rm iw}$, for which there is a large uncertainty. Theoretical approaches have been developed to estimate $\sigma_{\rm iw}$ however they are mostly applicable to low undercooling (e.g., Digilov, 2004; Spaepen, 1994) and $\sigma_{\rm iw}$ is in general found by fitting experimental measurements of $J_{\rm hom}$ (e.g., Murray et al., 2010a; Khvorostyanov and Curry, 2004; Marcolli et al., 2007). Two approaches are employed to parameterize $\sigma_{\rm iw}$. Following Murray et al. (2010a), the following correlation was used to describe $\sigma_{\rm iw}$,

$$\sigma_{\mathrm{iw}}(T) = 0.0229\left(\frac{T}{236.8}\right)^{0.97} \quad (\mathrm{J\ m^{-2}}) \tag{26}$$

With T in K. The parameters of the correlation in Eq. (26) were slightly modified to match the freezing point of pure water measured by Koop et al. (2000). The model presented in Section 2 however indicates that besides T, σ_{iw} must also depend on a_w since the presence of the solute in the interface layer modifies the interfacial energy. To account for this, a correlation for σ_{iw} was obtained by fitting Eq. (23) to the data of Koop et al. (2000) in the form,

$$\sigma_{\mathrm{iw}}(T, a_w) = 0.00211 - 0.0513 a_w + 3.04 \times 10^{-4} T \quad (\mathrm{J\ m^{-2}}) \tag{27}$$

With $180 < T < 273$ in K. The linear dependency of σ_{iw} on T is consistent with theoretical studies (Spaepen, 1994; Pruppacher and Klett, 1997). In agreement with experimental measurements (Pruppacher and Klett, 1997; Digilov, 2004), Eq. (27) predicts $\sigma_{\mathrm{iw}} = 33.9$ J m^{-2} for $T = 273$ K and $a_w = 1$.

3 Discussion

3.1 Nucleation Rate

Figure 2 shows the nucleation rate calculated from the NENT and CNT models, i.e., Eqs. (20) and (23). For NENT, the surface area parameter, s, in Eq. (19) was set to 1.105, that is, the ice germ structure is assumed to lie somewhere between a bcc ($s = 1.12$) and a hcp ($s = 1.109$) crystal, justified on experimental studies showing that ice forms as a stacked disordered structure (Malkin et al., 2012). The values used for the parameters of Eqs. (19) and (20) are listed in Table 1. J_{hom} from the empirical correlations of Koop et al. (2000) and Murray et al. (2010a) is also shown in Fig. 2. Murray et al. (2010a) compared experimentally determined nucleation rates from several sources and found about a factor of 10 variation in J_{hom} of pure water. The correlation of Murray et al. (2010a) was therefore included in Fig. 2 for reference, although it is only applicable around 236 K. CNT results are shown using Eqs. (26) and (27) to calculate σ_{iw}.

The median freezing temperature, T_{med}, was calculated by solving,

$$J_{\mathrm{hom}}(T_{\mathrm{med}}) \Delta t v_{\mathrm{d}} = 1 \tag{28}$$

where Δt is the experimental time scale v_{d} the droplet volume. Equation (28) is a result of the nucleation dispersion theory (Barahona, 2012) and indicates that half of the droplets in a population will freeze when there is on average one ice germ per droplet produced during Δt. T_{med} is calculated by numerical iteration and assuming $\Delta t = 10$ s and a droplet diameter of 10 μm, selected to match to the conditions used by Koop et al. (2000).

There is overlap between all the curves of Fig. 2 for T around 236 K, that is, near the homogeneous freezing T of pure water ($a_w = 1$). This is in agreement with the study of Murray et al. (2010a) showing that most models predict similar $J_{\rm hom}$ for pure water. However for $T < 236$ K and for $a_w < 1$, Fig. 2 shows significant differences in predicted nucleation rates. At constant a_w, $J_{\rm hom}$ for NENT increases more rapidly as T decreases than for CNT, indicating a more rapid decrease in $\Delta G_{\rm nuc}$ in NENT. $J_{\rm hom}$ for NENT also increases more quickly than for K00 as T decreases, although the discrepancy remains within the typical scatter of experimentally determined $J_{\rm hom}$ (Murray et al., 2010b). When Eq. (27) is used to parameterize $\sigma_{\rm iw}$, $J_{\rm hom}$ from CNT shows good agreement with K00; this is however by design as K00 was used to generate Eq. (27). When Eq. (26) is used to parameterize $\sigma_{\rm iw}$, $J_{\rm hom}$ from CNT is much lower than predicted by either NENT or K00, and only at $a_w = 1$ $J_{\rm hom}$ from CNT agrees with experimental observations. Such high sensitivity to $\sigma_{\rm iw}$ is one of the main drawbacks of CNT.

At constant a_w, NENT and CNT show an initial increase in $J_{\rm hom}$ as T decreases however this tendency reverses at low T. This behavior is caused by an increase in $\Delta G_{\rm act}$ as T decreases, reducing $J_{\rm hom}$. As T decreases the role of activation of water molecules becomes increasingly more significant, limiting $J_{\rm hom}$. In contrast, the K00 parameterization shows a monotonically increase in $J_{\rm hom}$ as T decreases. A plausible explanation for this behavior may be found in the experimental method used to generate the K00 parameterization. Optical methods are accurate at low $J_{\rm hom}$ where the freezing of individual droplets can be easily discriminated. However as T decreases, high $J_{\rm hom}$ results in rapid freezing of the entire droplet population. Thus the maximum and subsequent reduction in $J_{\rm hom}$ as T decreases may be difficult to infer from observation of the freezing of single droplets. Thus it is likely that the K00 parameterization overestimates the highest values of $J_{\rm hom}$. Numerical test (not shown) suggest this may lead to overestimation of droplet freezing fractions particularly for small droplets, although it may have a limited impact in ambient clouds where freezing fractions are typically small (Barahona and Nenes, 2008).

3.2 Critical germ size

Figure 3 shows the critical germ size in terms of number of water molecules, calculated using NENT and CNT. According to the nucleation theorem (Kashchiev, 2000), n^* can also be determined directly from experimental results following,

$$n^* = -\frac{{\rm d}\Delta G_{\rm nuc}}{{\rm d}\Delta\mu_w} + \frac{\partial\Phi}{\partial\Delta\mu_w} \tag{29}$$

where Φ is the energy of formation of the interface, and $\Delta\mu_w = -k_{\rm B}T\ln\left(\frac{a_w}{a_{w,eq}}\right)$. Equation (29) can be simplified as (Kashchiev, 2000),

$$n^* = \frac{{\rm d}\ln J_{\rm hom}}{{\rm d}\ln a_w} - 1 \tag{30}$$

where it is assumed that Φ, or equivalently $\sigma_{\rm iw}$, does not depend on a_w. Using the K00 parameterization into Eq. (30) results in n^* between 400 and 600 molecules for T between 180 K and 236 K (Fig. 3). On the other hand, NENT (Eq. 18) predicts n^* around 300 for the same T interval and CNT around 100 (Eq. 25). A similar discrepancy was found by Ford (2001) who ascribed it to deficiencies in CNT. However NENT offers further insight into the origin of the differences in n^*.

Figure 4 suggests that around the median freezing a_w (defined in a similar way as in Eq. 28), $\frac{{\rm d}\ln J_{\rm hom}}{{\rm d}\ln a_w}$ for K00 is similar as for CNT (with $\sigma_{\rm iw}$ as defined in Eq. 27) and lower than for NENT. The fact that n^* is higher for K00 than for NENT (Fig. 3), even though $\frac{{\rm d}\ln J_{\rm hom}}{{\rm d}\ln a_w}$ is higher in the latter, is at odds with the predictions of Eq. (30). This picture can only be reconciled if $\frac{\partial\Phi}{\partial\Delta\mu_w}\neq 0$, that is, the interfacial energy must be a functional of a_w, which is also suggested by Eq. (19). This dependency is explicit in the NENT model (Section 2.1). In CNT, it is introduced by making $\sigma_{\rm iw}$ a function of a_w.

To explain the dependency of the interfacial energy on a_w one must consider the Gibbs model of the interface (Section 2.1). By introducing the arbitrary dividing surface, an excess number of molecules is created around the interface between the liquid and the solid (Hiemenz and Rajagopalan, 1997). This is typically dealt with by selecting the so-called equimolecular dividing surface (EDS), in which the interface has energy but its net molecular excess is zero (Kashchiev, 2000; Schay, 1976). However the EDS cannot be defined simultaneously for both, the solute and the solvent. In fact, using the EDS with respect to the solvent, as implicitly done in CNT, results in a molecular excess of solute at the interface. This explains the discrepancy in n^* between Eq. (30) and CNT. In Section 2 it is shown that it is advantageous to define the EDS with respect to the solute, and account explicitly for the excess of water molecules at the interface. Thus the consistency between the choice of the dividing surface and the molecular excess at the interface is explicit in NENT. This picture also implies that Eq. (29) (which does not depend on the choice of the dividing surface) instead of Eq. (30), must be used in the analysis of ice nucleation data.

3.3 Median Freezing Temperature

Finally we investigate whether the model presented in Section 2 is able to explain the water activity criteria of Koop et al. (2000). Figure 5 shows the median freezing T defined by Eq. (28), calculated using K00, CNT and NENT. For CNT using Eq. (27) results in agreement with K00, which however is by design as $T_{\rm med}$ predicted by K00 was used to specify $\sigma_{\rm iw}$ (Eq. 27). Using $\sigma_{\rm iw}$ from Eq. (26) which is based on a fit to observed $T_{\rm med}$ at $a_w=1$ results in overprediction of $T_{\rm med}$ for $a_w<1$. $T_{\rm med}$ from K00 and NENT overlap down to 190 K (Fig. 5). Since no data from K00 are used in NENT, the model developed here constitutes the first theoretical explanation of the results of Koop et al. (2000).

The shift in water activity, $\Delta a_w = a_w - a_{w,eq}$, can be obtained by solving,

$$k_{\mathrm{B}}T\ln(J_0\Delta t v_{\mathrm{d}}) - \frac{4}{27}\frac{\{1.46s[\Delta h_f - 1.46sk_{\mathrm{B}}T\ln(a_{w,eq}+\Delta a_w)]\}^3}{\left\{k_{\mathrm{B}}T\ln\left[\frac{(a_{w,eq}+\Delta a_w)^2}{a_{w,eq}}\right]\right\}^2} = 0 \tag{31}$$

Equation (31) was obtained by replacing Eq. (20) into Eq. (28). Since the roots of Eq. (31) determine T_{med}, it is termed the characteristic freezing function .

Inspection of Eq. (31) shows that it is a function of T only, since the a_w dependency is removed by application of Eq. (28). Thus, the roots of Eq. (31) are determined by the value of Δa_w. Figure (6) shows that Eq. (31) only has real solutions in the interval $185 < T < 238$ K over a very narrow set of values of Δa_w, i.e., $0.298 < \Delta a_w < 0.304$. This is the origin of the water activity criteria since such variation in Δa_w is well within experimental uncertainty. An interesting feature of Eq. (31) is that it produces similar $T - a_w$ curves for different Δa_w values. This means that the multiple roots of Eq. (31) are located at similar T_{med} for different values of Δa_w, and always fall on the same curve.

Figure 6 shows that Eq. (31) constitutes a theoretical derivation of the water activity criteria. Δa_w can be easily obtained by numerical iteration of Eq. (31). However at $a_w = 1$, Eq. (31) is greatly simplified and Δa_w can be found by direct analytical solution, in the form,

$$\Delta a_w = 1 - \exp\left[-\frac{2}{3\sqrt{3\ln(J_0\Delta t v_{\mathrm{d}})}}\left(\frac{\Delta h_f}{k_{\mathrm{B}}T^*}\right)^{3/2}\right] = 0.2981 \tag{32}$$

where $T^* = 236.03$ is the median freezing temperature at $a_w = 1$. The value of Δa_w in Eq. (32) was obtained using the parameters of Table 1 calculated at T^*. Δa_w is very close to the experimental value of 0.302 found by Koop et al. (2000). For $T > 190$ K, Δa_w calculated from Eq. (31) is fairly constant (being 0.300 at $T = 190$ K). For $T < 190$ there is a slight increase in Δa_w reaching about 0.31 at $T = 180$ K. This increase is due to the increase in ΔG_{act} at low T. J_{hom} at very low T is still uncertain, since factors like the formation of glasses (Murray et al., 2010b) and the formation of highly concentrated brines within droplets may play a role (Bogdan and Molina, 2010). The accuracy of K00 at very low T has also been questioned (Swanson, 2009).

The preexpoential factor in Eq. (21) is almost constant between 180 K and 236 K. That is, the flux of molecules to the germ is controlled by ΔG_{act}. In fact, by replacing Eq. (19) into Eq. (20) and then into Eq. (28), we obtain after rearranging,

$$\frac{\Delta G_{\mathrm{nuc}} + \Delta G_{\mathrm{act}}}{T} \approx \mathrm{constant} \tag{33}$$

Thus an increase ΔG_{act} is balanced by a decrease in ΔG_{nuc}, i.e., the increase in the driving force for nucleation at low T makes up for the decrease in the mobility of water molecules. Since ΔG_{nuc} can be defined over a pure thermodynamic basis (Section 2), Eq. (33) suggest that ΔG_{act} and the kinetic term in Eq. (20) may also admit a thermodynamic description.

4 Conclusions

The model presented in Section 2 constitutes a new theory of nucleation that does not use the interfacial tension as defining parameter. It is therefore free from biases induced by uncertainties in the parameterization of σ_{iw}. Instead, an expression for the interfacial energy was developed directly using thermodynamic principles. The new theory is based on a conceptual model in which the interface is considered to be made of "water molecules trapped by the solid matrix". It also accounts for the finite droplet size leading to changes in the composition of the liquid phase upon nucleation. Since it places emphasis on the increase in order and the reduction in entropy across the interface, the new model has been termed the Neg-Entropic Theory of Nucleation, NENT.

Comparison against experimental results showed that the new theory is able to reproduce measured nucleation rates and is capable of explaining the observed constant shift in water activity between melting and nucleation (Koop et al., 2000). The constant water activity shift originates because the median freezing temperature only exist for a very narrow range of Δa_w values (Eq. 31). More fundamentally, NENT shows that the effect of water activity on nucleation is a manifestation of the entropic barrier to the formation of the germ. An analytical expression for Δa_w was derived and was shown to agree well with the experimental value measured by Koop et al. (2000). This constitutes the first theoretical derivation of the water activity criteria found by Koop et al. (2000).

The new theory suggests that to reconcile experimental results and theoretical models the interfacial energy must depend on a_w. This is implicit in the development of NENT, however is missing in CNT. The dependency of J_{hom} on a_w originates from the excess concentration of either solute of solvent when the dividing surface is defined. Such excess is present even if the EDS is defined with respect to the solvent. It was shown that it is advantageous to define the EDS with respect to the solute because the resulting expressions are independent of the nature of the solute, and therefore consistent with experimental observations. Although such considerations are neglected in CNT, it was shown that CNT can be corrected by allowing σ_{iw} to depend on a_w, for which a new empirical correlation was developed.

Analysis of the new theory suggested that the temperature dependency of both the kinetic and thermodynamic terms plays a significant role in defining J_{hom} and T_{med}. It was shown that around T_{med} the increase in ΔG_{act} as T decreases is compensated by a decrease in ΔG_{nuc}. Thus an increased driving force for nucleation compensates the slower molecular diffusion at low T. Such coupling between kinetic and thermodynamics during nucleation suggests that a thermodynamic description of the preexponential factor (Eq. 20) may be possible.

Some disparity was found between the K00 parameterization and NENT for $T < 190$ K. This may be ascribed to non-equilbrium effects and the possible formation of glasses at low T. Also the solute term in Eq. (7) may become important as a_w decreases. Further research is required to elucidate the mechanism of freezing at such low T. The model presented here emphasizes the entropic nature of homogeneous nucleation. Molecular simulations may shed further light on the role of entropy

changes across the interface on ice nucleation. Measurements of the interface thickness would also help elucidate the role of the ice crystal geometry (represented by the constant s in Eq. 15) in determining $J_{\rm hom}$. The new theory is also suitable to describe heterogeneous freezing, particularly in the immersion mode. This will be addressed in future studies.

The theory presented here reconciles theoretical an experimental results. It will also help reduce the uncertainty in $J_{\rm hom}$ associated with the parameterization of $\sigma_{\rm iw}$ in theoretical models. It offers for the first time a thermodynamically consistent explanation of the effect of water activity on ice nucleation. Its relative simplicity makes it suitable to describe ice nucleation in the atmosphere, and may lead to a better understanding of the formation of ice clouds and their parameterization in atmospheric models.

Acknowledgements. Donifan Barahona was supported by the NASA Modeling, Analysis and Prediction program under WBS 802678.02.17.01.07. The author thanks Athanasios Nenes for his comments on the manuscript.

References

Baker, M. and Baker, M.: A new look at homogeneous freezing of water, Geophys. Res. Lett., 31, 2004.

Barahona, D.: On the ice nucleation spectrum, Atm. Chem. Phys., 12, 3733–3752, doi:10.5194/acp-12-3733-2012, http://www.atmos-chem-phys.net/12/3733/2012/, 2012.

Barahona, D. and Nenes, A.: Parameterization of cirrus formation in large scale models: Homogeneous nucleation, J. Geophys. Res., 113, D11 211, doi:10.1029/2007JD009355, 2008.

Barahona, D. and Nenes, A.: Dynamical states of low temperature cirrus, Atmos. Chem. Phys., 11, 3757–3771, doi:10.5194/acp-11-3757-2011, 2011.

Barahona, D., Rodriguez, J., and Nenes, A.: Sensitivity of the global distribution of cirrus ice crystal concentration to heterogeneous freezing, J. Geophys. Res., 15, D23 213, doi:10.1029/2010JD014273, 2010.

Barahona, D., Molod, A., Bacmeister, J., Nenes, A., Gettelman, A., Morrison, H., Phillips, V., and Eichmann, A.: Development of two-moment cloud microphysics for liquid and ice within the NASA Goddard earth observing system model (GEOS-5), Geos. Mod. Dev., p. Submitted, 2013.

Bauerecker, S., Ulbig, P., Buch, V., Vrbka, L., and Jungwirth, P.: Monitoring ice nucleation in pure and salty water via high-speed imaging and computer simulations, J. Phys. Chem. C, 112, 7631–7636, 2008.

Black, S.: Simulating nucleation of molecular solids, Proc. Royal Soc. A, 463, 2799–2811, 2007.

Bogdan, A. and Molina, M.: Aqueous aerosol may build up an elevated upper tropospheric ice supersaturation and form mixed-phase particles after freezing, J. Phys. Chem. A, 114, 2821–2829, 2010.

Bourne, J. and Davey, R.: The role of solvent-solute interactions in determining crystal growth mechanisms from solution: I. The surface entropy factor, J. Crystal Growth, 36, 278–286, 1976.

Chen, J.-P. and Crutzen, P. J.: Solute effects on the evaporation of ice particles, J. Geophys. Res., 99, 18 847–18 859, 1994.

Digilov, R. M.: Semi-empirical model for prediction of crystal–melt interfacial tension, Surface Sci., 555, 68–74, 2004.

Ford, I. J.: Properties of ice clusters from an analysis of freezing nucleation, J. Phys. Chem. B, 105, 11 649–11 655, 2001.

Fu, Q.: An accurate parameterization of the solar radiative properties of cirrus clouds for climate models, J. Clim., 9, 2058–2082, 1996.

Gettelman, A., Liu, X., Barahona, D., Lohmann, U., and Chen, C.: Climate impacts of ice nucleation, J. Geophys. Res., 117, doi:10.1029/2012JD017950, 2012.

Gibbs, J. W., Bumstead, H. A., and Longley, W. R.: The collected works of J. Willard Gibbs, vol. 1, Longmans, Green and Company, 1928.

Hartmann, D., Holton, J., and Fu, Q.: The heat balance of the tropical tropopause, cirrus, and stratospheric dehydration, Geophys. Res. Lett., 28, 1969–1972, 2001.

Haymet, A. and Oxtoby, D. W.: A molecular theory for the solid–liquid interface, J. Chem. Phys., 74, 2559, 1981.

Henson, B. and Robinson, J.: Dependence of quasiliquid thickness on the liquid activity: A bulk thermodynamic theory of the interface, Phys. Rev. Lett., 92, 246 107, 2004.

Hiemenz, P. C. and Rajagopalan, R.: Principles of Colloid and Surface Chemistry, revised and expanded, vol. 14, CRC Press, 1997.

Jensen, E. and Pfister, L.: Transport and freeze-drying in the tropical tropopause layer, J. Geophys. Res., 109, D02 207; doi:10.1029/2003JD004 022, 2004.

Jensen, E. J., Toon, O. B., and Hamill, P.: Homogeneous freezing nucleation of stratospheric solution droplets, Geophys. Res. Lett., 18, 1857–1860, 1991.

Jian, Z., Kuribayashi, K., and Jie, W.: Solid-liquid interface energy of metals at melting point and undercooled state, Materials Trans., 43, 721–726, 2002.

Johari, G., Fleissner, G., Hallbrucker, A., and Mayer, E.: Thermodynamic continuity between glassy and normal water, J. Phys. Chem., 98, 4719–4725, 1994.

Kärcher, B. and Lohmann, U.: A parameterization of cirrus cloud formation: homogeneous freezing including effects or aerosol size, J. Geophys. Res., 107, 4698, doi:10.1029/2001JD001 429, 2002.

Karim, O. A. and Haymet, A.: The ice/water interface: A molecular dynamics simulation study, J. Chem. Phys., 89, 6889, 1988.

Kashchiev, D.: Nucleation: basic theory with applications, Butterworth Heinemann, 2000.

Khvorostyanov, V. I. and Curry, J. A.: Thermodynamic theory of freezing and melting of water and aqueous solutions, J. Phys. Chem. A, 108, 11 073–11 085, 2004.

Koop, T., Luo, B., Tslas, A., and Peter, T.: Water activity as the determinant for homogeneous ice nucleation in aqueous solutions, Nature, 406, 611–614, 2000.

Laaksonen, A., Talanquer, V., and Oxtoby, D. W.: Nucleation: Measurements, theory, and atmospheric applications, Ann. Rev. Phys. Chem., 46, 489–524, 1995.

Liu, X. and Penner, J.: Ice nucleation parameterization for global models, Meteorol. Z., 14, 499–514, 2005.

Liu, X., Penner, J., Ghan, S., and Wang, M.: Inclusion of ice microphysics in the NCAR Community Atmospheric Model version 3 (CAM3), J. Clim., 20, 4526–4547, 2007.

Lohmann, U. and Feichter, J.: Global indirect aerosol effects: a review, Atmos. Chem. Phys., 5, 715–737, 2005.

MacKenzie, A.: Are the (Solid-Liquid) Kelvin Equation and the Theory of Interfacial Tension Components Commensurate?, J. Phys. Chem. B, 101, 1817–1823, 1997.

Malkin, T. L., Murray, B. J., Brukhno, A. V., Anwar, J., and Salzmann, C. G.: Structure of ice crystallized from supercooled water, PNAS, 109, 1041–1045, 2012.

Marcolli, C., Gedamke, S., Peter, T., and Zobrist, B.: Efficiency of immersion mode ice nucleation on surrogates of mineral dust, Atmos. Chem. Phys., 7, 5081–5091, 2007.

Matsumoto, M., Saito, S., and Ohmine, I.: Molecular dynamics simulation of the ice nucleation and growth process leading to water freezing, Nature, 416, 409–413, 2002.

Murphy, D. and Koop, T.: Review of the vapour pressures of ice and supercooled water for atmospheric applications, Q. J. R. Meteorol. Soc., 131, 1539–1565, 2005.

Murray, B., Broadley, S., Wilson, T., Bull, S., Wills, R., Christenson, H., and Murray, E.: Kinetics of the homogeneous freezing of water, Phys. Chem. Chem. Phys., 12, 10 380–10 387, 2010a.

Murray, B., Wilson, T., Dobbie, S., Cui, Z., Al-Jumur, S., Mähler, O., Schnaiter, M., Wagner, R., Benz, S., Niemand, M., Saathoff, H., Ebert, V., Wagner, S., and Krcher, B.: Heterogeneous nucleation of ice particles on glassy aerosol under cirrus conditions, Nature Geosci., 3, 233–237, 2010b.

Pruppacher, H. and Klett, J.: Microphysics of clouds and precipitation, Kluwer Academic Publishers, Boston, MA, 2nd edn., 1997.

Reinhardt, A. and Doye, J. P.: Note: Homogeneous TIP4P/2005 ice nucleation at low supercooling, J. Chem. Phys., 139, 096 102, 2013.

Schay, G.: A comprehensive presentation of the thermodynamics of adsorption excess quantities, Pure Appl. Chem., 48, 393–400, 1976.

Spaepen, F.: A structural model for the solid-liquid interface in monatomic systems, Acta Metallurgica, 23, 729–743, 1975.

Spaepen, F.: Homogeneous nucleation and the temperature dependence of the crystal-melt interfacial tension, Solid State Phys., 47, 1–32, 1994.

Swanson, B. D.: How Well Does Water Activity Determine Homogeneous Ice Nucleation Temperature in Aqueous Sulfuric Acid and Ammonium Sulfate Droplets?, J. Atm. Sci., 66, 741–754, 2009.

Tabazadeh, A., Jensen, E., and Toon, O.: A model description for cirrus cloud nucleation from homogeneous freezing of sulfate aerosols, J. Geophys. Res., 102, 23 485–23 850, 1997.

Wang, B. and Knopf, D. A.: Heterogeneous ice nucleation on particles composed of humic-like substances impacted by O_3, J. Geophys. Res., 116, D03 205, 2011.

Wu, D. T., Gránásy, L., and Spaepen, F.: Nucleation and the Solid–Liquid Interfacial Free Energy, MRS Bull., 29, 945–950, 2004.

Zobrist, B., Koop, T., Luo, B., Marcolli, C., and Peter, T.: Heterogeneous ice nucleation rate coefficient of water droplets coated by a nonadecanol monolayer, J. Phys. Chem. C, 111, 2149–2155, 2007.

Table 1. List of symbols.

a_w, a_y	Activity of water and solute, respectively
$a_{w,eq}$	Equilibrium a_w between bulk liquid and ice (Koop et al., 2000)
G	Gibbs free energy
h	Planck's constant
$h_{w,s}$, $h_{w,ls}$	Partial molar enthalpy of water in ice and at the interface, respectively
J_0	Preexponential factor
$J_{\rm hom}$	Nucleation rate
$k_{\rm B}$	Boltzmann constant
n	Total number of molecules in the solid germ
$n*$	Critical germ size
n_s, n_{ls}	Number of molecules in the bulk of the solid and in the interface, respectively
N_c	Number of atoms in contact with the ice germ, 5.85×10^{18} m^{-2} (Pruppacher and Klett, 1997)
N_w, N_y	Total number of water and solute molecules, respectively
$p_{\rm s,w}$, $p_{\rm s,i}$	Liquid water and ice saturation (Murphy and Koop, 2005)
s	Geometric constant relating n and n_{ls}
$S_{\rm i}$	Saturation ratio with respect to ice
$s_{w,s}$, $s_{w,ls}$	Partial molar entropy of water in bulk ice and at the interface, respectively
T	Temperature
$T_{\rm med}$	Median freezing T
$v_{\rm d}$	Droplet volume
v_w	Molecular volume of water in ice (Zobrist et al., 2007)
X_w, X_y	Molar fraction of water and solute, respectively
Z	Zeldovich factor
$\Delta G_{\rm act}$	Activation energy of liquid water (Zobrist et al., 2007)
$\Delta G_{\rm nuc}$	Nucleation work
$\Delta G_{\rm sln}$	Change in free energy of the bulk solution during nucleation
$\Delta h_{w,ls}$	Excess enthalpy of the interface
Δh_f	Heat of fusion of water [a]
Δt	Experimental time scale
Δa_w	$a_w - a_{w,eq}$
Φ	Energy of formation of the interface
Γ_w, Γ_y	Molecular surface excess of water and solute, respectively
μ_w, μ_y	Chemical potential of water and solute, respectively
$\mu_{w,ls}$	Chemical potential of water at the interface
$\mu_{w,s}$	Chemical potential of bulk ice
ρ_w, ρ_i	Bulk density of liquid water and ice, respectively (Pruppacher and Klett, 1997)
$\sigma_{\rm iw}$	Ice-liquid interfacial energy
Ω_g	Ice germ surface area

[a] From the data of Johari et al. (1994) the following fit was obtained: $\Delta h_f = 7.50856 \times 10^{-7} T^5 - 8.40025 \times 10^{-4} T^4 + 0.367171 T^3 - 78.1467 T^2 + 8117.02 T - 3.29032 \times 10^5$ (J mol^{-1}) for T between 180 K and 273 K.

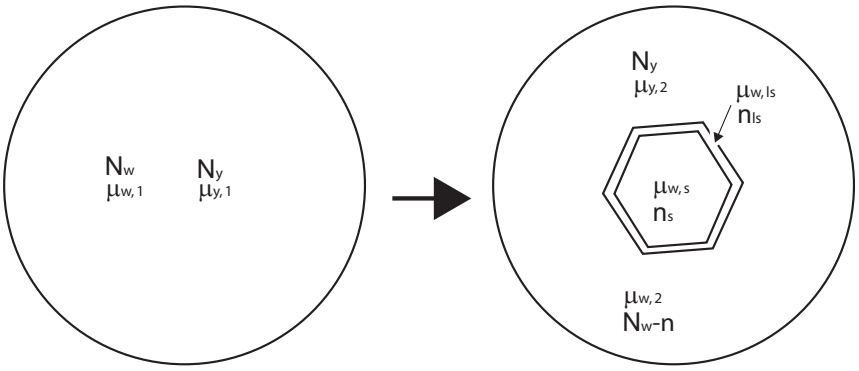

Fig. 1. Scheme of the formation of an ice germ from a liquid phase.

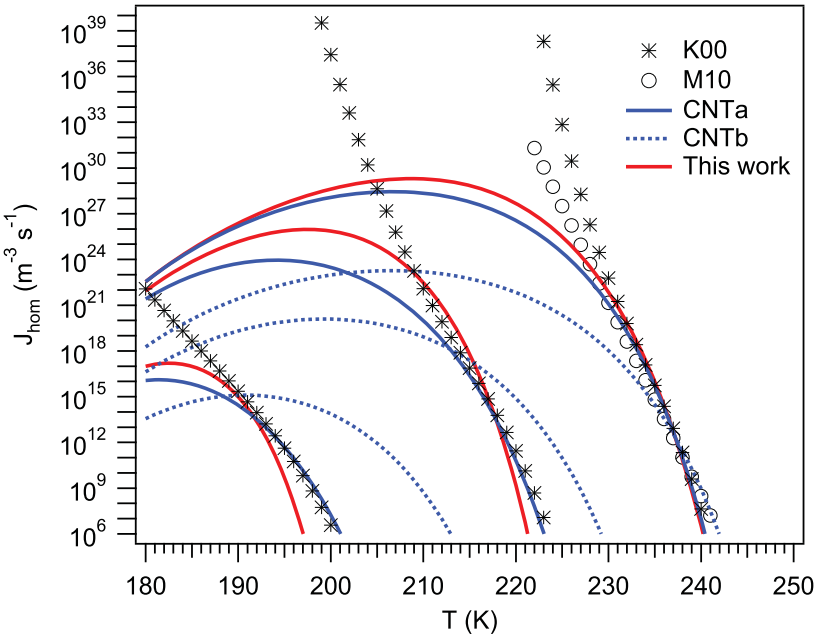

Fig. 2. Homogeneous nucleation rate. K00 and M10 refer to results obtained using the correlations of Koop et al. (2000) and Murray et al. (2010a), respectively. For CNT σ_{iw} was calculated using either Eq. (27) (line CNTa) or Eq. (26) (line CNTb). Lines are grouped by increasing water activity: $a_w = 0.8$,0.9 and 1.0, from left to right, respectively.

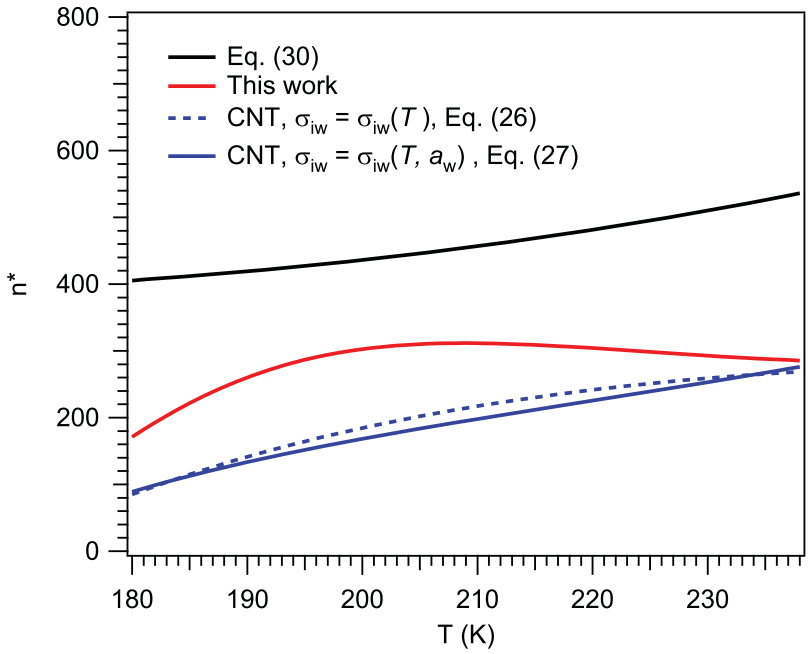

Fig. 3. Critical germ size, n^*.

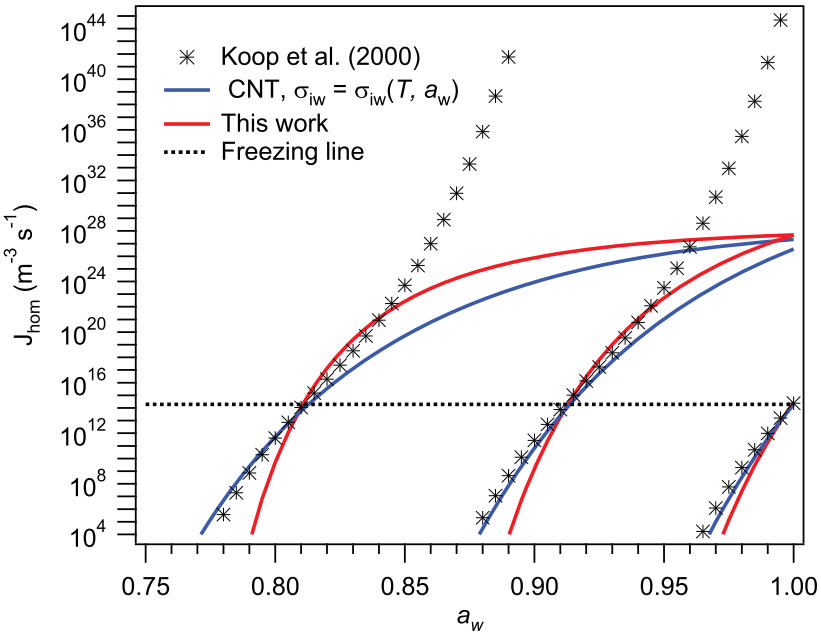

Fig. 4. Homogeneous nucleation rate. The freezing line was calculated using Eq. (28). Lines are grouped by temperature: $T = 195, 220$ and 236 K, from left to right, respectively.

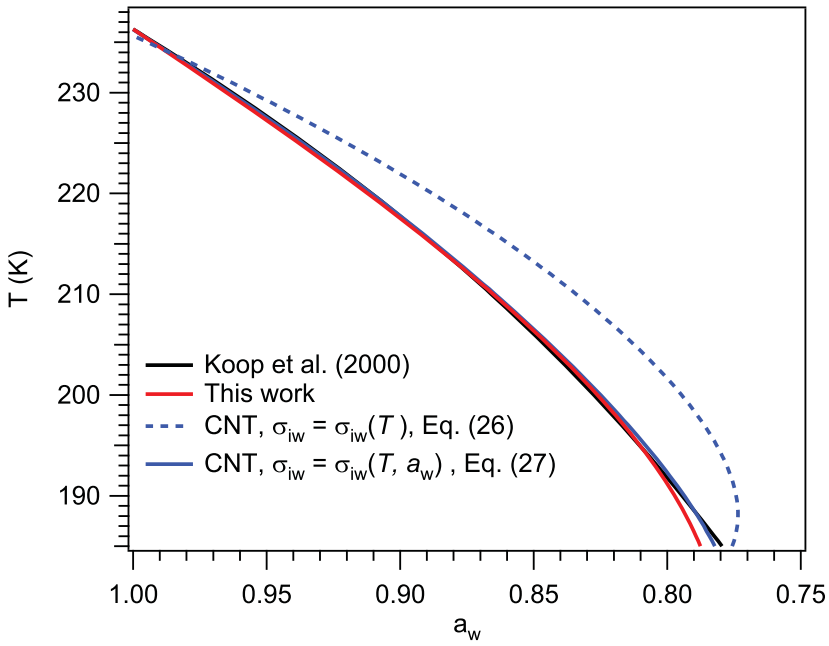

Fig. 5. Median freezing temperature for homogeneous nucleation.

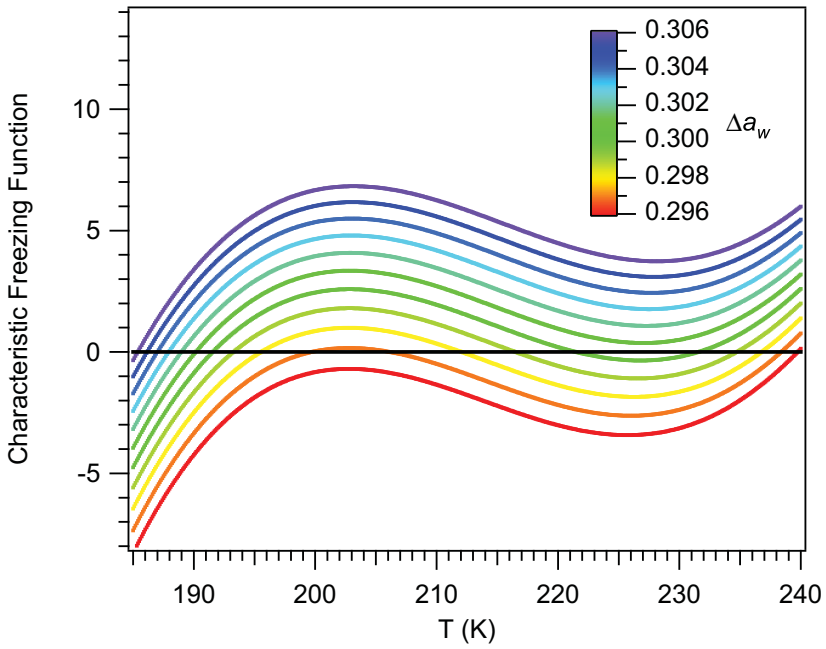

Fig. 6. Characteristic freezing function, Eq. (31).